Tensor Product model based PID controller optimisation for propofol administration

József Kuti, Péter Galambos

Antal Bejczy Center for Intelligent Robotics, Óbuda University, Bécsi út 96/B. H-1034 Budapest, Hungary

Abstract: This study investigates the computer-regulated propofol administration in anesthesia during medical interventions considering output feedback and robust PID control. The paper applies the Affine Tensor Product Model Transformation to derive the appropriate polytopic quasi-LPV representation of the closed-loop dynamics. This model form enables the use of LMI-based optimisation techniques to evaluate the closed loop performance. Despite the highly non-convex nature of this output feedback problem, the PID gains can be locally tuned through simplex optimisation. The proposed method provides a systematic way of tuning PID-controlled propofol administration for individual patients with theoretically established worst-case performance measures.

Keywords: Modelling and Control of Biomedical Systems; Control Design; Optimal Control, Anesthesia, Propofol administration

1. INTRODUCTION

Polytopic model-based control and especially the polytopic Tensor Product (TP) model-based control aims to analyze and synthesize control loops for parameter-dependent and nonlinear plants given as Linear Parameter Varying (LPV) or quasi-LPV forms (see Boyd (1994); Baranyi et al. (2013)). The purpose is mainly to derive a convex optimisation program, which can be solved via interior point methods (see Nesterov and Nemirovsky (1988)).

The design of output feedback methods, - like PID control, which has great practical relevance - are usually highly non-convex problems. There are different approaches to convexify the problems to apply local optimisations see Qiu et al. (2013); Crusius and Trofino (1999); Bianchi et al. (2008); Thevenet et al. (2004); Hassibi et al. (1999).

In this paper, we consider the propofol administration problem during anesthesia to achieve the appropriate depth of hypnosis (DOH) without considering the remifentanil that is applied to ensure pain management. Clinical tests showed that the adequately designed dynamical model-based controller could perform better than the manual administration (see Hemmerling et al. (2010)). The depth of hypnosis can be measured through Bispectral Monitor index (see Orliaguet et al. (2015)), M-Entropy and wavelet-based indices (WAV_{CNS}, WAV_{ANS}). The wavelet-based indices allowed to measure the depth of hypnosis without delay, and its dynamics shows LTI characteristics (see Pilge et al. (2006); Bibian and Zikov (2011); Bibian et al. (2011)).

The depth of hypnosis is controlled via PID controller by Padula et al. (2015); Van Heusden et al. (2014) according to the practical opportunities, patient specific controllers were designed via LPV/LMI framework by Lin et al. (2008), MPC controller is proposed by Nascu et al. (2015) and the opportunities of robust fixed point transformation is also considered by Tar et al. (2016); Dineva et al. (2016).

In this study, we consider the local optimisation of PID controller by applying LMI-based control analysis on the polytopic TP model of the regulated propofol administration. First, a qLPV model is derived, that gives an exact representation of the investigated system including the nonlinearities, saturation, time-delay, and sampling according to the desired equilibrium state. Then the polytopic TP model is constructed with appropriately chosen parameter sets. The closed-loop system can be obtained with the given PID gains. Finally, the closed-loop performance can be evaluated via convex optimisation, and based on the results the PID gains can be tuned locally to improve the performance.

2. BASIC CONCEPTS

2.1 Propofol administration and DOH measurement model

This subsection describes the model of propofol administration that is considered in this study. The model is recalled based on Ionescu et al. (2014); Padula et al. (2015); Van Heusden et al. (2014)) and for DOH measurement via NeuroSENSE NS-701 Bibian et al. (2011); Bibian and Zikov (2011).

The pharmacokinetic compartment of propofol administration is usually modeled as a third-order transfer function. It is described in state-space form as

$$\dot{C}_p = -(k_{10} + k_{12} + k_{13})C_p + k_{21}C_m + k_{31}C_f + \frac{u}{V_1}, \quad (1)$$

$$\dot{C}_m = k_{12}C_p - k_{21}C_m, \quad (2)$$

$$\dot{C}_f = k_{13}C_p - k_{31}C_f, \quad (3)$$

where C_p denotes the propofol concentration in the intervascular blood plasma ($[mg/L]$), C_m the concentration

Parameter	Value
$V_1[L]$	4.27
$V_2[L]$	$18.9 - 0.391(age[year] - 53)$
$V_3[L]$	2.38
$lbm_{males}[kg]$	$1.1weight[kg] - 128\frac{weight[kg]^2}{height[cm]^2}$
$lbm_{females}[kg]$	$1.07weight[kg] - 148]\frac{weight[kg]^2}{height[cm]^2}$
$C_{l1}[L/min]$	$1.89 + 0.0456(weight[kg] - 77)$ $-0.0681(lbm[kg] - 59)$ $+0.0264(height[cm] - 177)$
$C_{l2}[L/min]$	$1.29 - 0.024(age[year] - 53)$
$C_{l3}[L/min]$	0.836
k_{10}, k_{12}, k_{13} $[min^{-1}]$	$\frac{C_{l1}}{V_1}$, $\frac{C_{l2}}{V_1}$, $\frac{C_{l3}}{V_1}$
k_{21}, k_{31} $[min^{-1}]$	$\frac{C_{l2}}{V_2}$, $\frac{C_{l3}}{V_3}$
k_d, k_a $[min^{-1}]$	0.456
T_d [s]	5

Table 1. Parameters of the PK-PD model (Ionescu et al. (2014))

#	Age	H[cm]	W[kg]	Gender	C_{E50}	γ	E_0	E_{max}
1	40	163	54	F	6.33	2.24	98.8	94.10
2	36	163	50	F	6.76	4.29	98.6	86.00
3	28	164	52	F	8.44	4.10	91.2	80.70
4	50	163	83	F	6.44	2.18	95.9	102.0
5	28	164	60	M	4.93	2.46	94.7	85.30
6	43	163	59	F	12.00	2.42	90.2	147.0
7	37	187	75	M	8.02	2.10	92.0	104.0
8	38	174	80	F	6.56	4.12	95.5	76.40
9	41	170	70	F	6.15	6.89	89.2	63.80
10	37	167	58	F	13.70	1.65	83.1	151.0
11	42	179	78	M	4.82	1.85	91.8	77.90
12	34	172	58	F	4.95	1.84	96.2	90.80
13	38	169	65	F	7.42	3.00	93.1	96.58

Table 2. Considered set of patients (Padula et al. (2015))

in the muscles ($[mg/L]$) and C_f in the fat ($[mg/L]$), the propofol infusion denoted by u and given in $[mg/min]$. The related coefficients are detailed in Table 1.

The pharmacodynamic model of the drug is a delayed first order system

$$C_e(s) = e^{-T_d s}\frac{k_a}{s + k_d}C_p(s). \quad (4)$$

The saturation is described by the Hill-function and influenced by the nociceptive stimulations (d) of the surgery as

$$E(t) = E_0 - E_{max}\frac{C_e(t)^\gamma}{C_{E50}^\gamma + C_e(t)^\gamma} + d(t), \quad (5)$$

where the parameters are patient-dependent. A few typical values for benchmark purposes are recited in Table 2.

The value E describes the DOH range from $0-100$, where 0 corresponds to isoelectric EEG, $90-100$ corresponds to awakeness, and $40-60$ is the desired, typical range for anesthesia.

The NeuroSENSE NS-701 Monitor (NeuroWave Systems Inc, OH) provides the WAV_{CNS} (Wavelet-based Anesthetic Value for Central Nervous System) as a delay-free, time-invariant and linear quantifier of cortical activity. Its dynamics can be described via a two-order transfer function as

$$WAV_{CNS}(s) = H(s)E(s), \quad (6)$$

where

$$H(s) = \frac{0.0115}{s^2 + 0.1841s + 0.0115}. \quad (7)$$

2.2 LPV/qLPV modelling

The discrete-time, linear, parameter-varying models will be denoted as

$$\begin{bmatrix}\mathbf{x}(T+1)\\ \mathbf{y}(T)\\ \mathbf{z}(T)\end{bmatrix} = \underbrace{\begin{bmatrix}\mathbf{A}(\mathbf{p}) & \mathbf{B}_u(\mathbf{p}) & \mathbf{B}_d(\mathbf{p})\\ \mathbf{C}_y(\mathbf{p}) & \mathbf{D}_{yu}(\mathbf{p}) & \mathbf{D}_{yd}(\mathbf{p})\\ \mathbf{C}_z(\mathbf{p}) & \mathbf{D}_{zu}(\mathbf{p}) & \mathbf{D}_{zd}(\mathbf{p})\end{bmatrix}}_{\mathbf{S}(\mathbf{p})}\begin{bmatrix}\mathbf{x}(T)\\ \mathbf{u}(T)\\ \mathbf{d}(T)\end{bmatrix}, \quad (8)$$

where $\mathbf{x}(T) \in \mathbb{R}^n$ denotes the state vector, $\mathbf{u}(T) \in \mathbb{R}^p$ is the input signal, $\mathbf{d}(T) \in \mathbb{R}^k$ are the disturbance, while $\mathbf{z}(T)$ is the performance channel. The size of parameter-dependent matrices are chosen accordingly.

For example, based on the Bounded Real Lemma, the stability and the disturbance rejection performance can be verified via convex optimisation, see Gahinet and Apkarian (1994).

Lemma 1. System (8) with $u = 0$ is stable, and $||\mathbf{D}_{zd}(\mathbf{p}) + \mathbf{C}_z(\mathbf{p})(s\mathbf{I} - \mathbf{A}(\mathbf{p}))^{-1}\mathbf{B}_d(\mathbf{p})||_\infty < \gamma$ if there exists a function $\mathbf{X}(\mathbf{p})$ such that

$$\begin{bmatrix}-\mathbf{X}(\mathbf{p}) & \mathbf{X}(\mathbf{p})\mathbf{\Phi}(\mathbf{p}) & \mathbf{X}(\mathbf{p})\mathbf{B}_d(\mathbf{p}) & \mathbf{0}\\ \mathbf{\Phi}^T(\mathbf{p})\mathbf{X}(\mathbf{p}) & -\mathbf{X}(\mathbf{p}) & \mathbf{0} & \mathbf{C}_z^T(\mathbf{p})\\ \mathbf{B}_d^T(\mathbf{p})\mathbf{X}(\mathbf{p}) & \mathbf{0} & -\gamma\mathbf{I} & \mathbf{D}^T(\mathbf{p})\\ \mathbf{0} & \mathbf{C}_z(\mathbf{p}) & \mathbf{D}(\mathbf{p}) & -\gamma\mathbf{I}\end{bmatrix} \prec 0 \quad (9)$$

for all considered $\mathbf{p}$.

The Linear Matrix Inequality based control design methodologies can be applied on nonlinear systems as well by rewriting them into the form of (8). It is called quasi-LPV model because the parameters depend on some of the state variables.

2.3 Polytopic TP model-based controller design

Consider the qLPV model (8) and its parameter dependent system matrix as a mapping from the investigated parameter domain

$$\Omega = [\underline{p}_1, \overline{p}_1] \times \dots [\underline{p}_K, \overline{p}_K] \quad (10)$$

to the space of system matrices ($\mathbb{S}$) as $\mathbf{S}(\mathbf{p}) : \Omega \to \mathbb{S}$.

By defining parameter sets as $\mathbf{p}^{(1)}$, $\mathbf{p}^{(2)}$, ... $\mathbf{p}^{(K)}$ from the scalar parameters and denoting the corresponding parameter domains by $\Omega_1, \Omega_1, \dots \Omega_K$, the Polytopic Tensor Product model can be defined as a form that is polytopic for all parameter sets. Polytopic TP model is defined as follows.

Definition 1. (Polytopic Tensor Product model). The LPV/qLPV model (8) with system matrix given as

$$\mathbf{S}(\mathbf{p}) = \mathcal{S} \bigboxtimes_{k=1}^{K} \mathbf{w}^{(k)}(\mathbf{p}^{(k)}) \quad (11)$$

in which the core tensor is on $\mathbb{S}$, it has sizes $(J_1 \times \dots \times J_K)$, and the J_k values are the number of vertices of the

$$\mathbf{S}(\mathbf{p}) = \sum_{j=1}^{J_k}\left(\mathcal{S}_{j_k=j} \bigboxtimes_{l=1, l\neq k}^{K} \mathbf{w}^{(l)}(\mathbf{p}^{(l)})\right) w_j^{(k)}(\mathbf{p}^{(k)}) \quad (12)$$

polytopic description, where the $w_1^{(k)}(\mathbf{p}^{(k)}), ..., w_{J_k}^{(k)}(\mathbf{p}^{(k)})$ weights denote convex combination for all $\mathbf{p}^{(k)} \in \Omega_k$, $k = 1..K$.

To derive Polytopic TP forms, the affine TP form is defined as a multi-affine description. It is based on an

affine Singular Value Decomposition (ASVD), that can be written for a vector function $\mathbf{f} : \Omega \to \mathbb{R}^A$ as

$$\mathbf{f}(\mathbf{p}) = \sum_{d=1}^{D} v_d(\mathbf{p})\mathbf{f}_d + \mathbf{f}_{D+1} = \sum_{d=1}^{D+1} v_d(\mathbf{p})\mathbf{f}_d, \quad (13)$$

where the $\mathbf{f}_d$ $(d = 1, ..., D)$ vectors are orthogonal and ordered by norm $(\sigma_1 \geq \sigma_2 \geq ... \geq \sigma_D > 0)$, and furthermore, $v_{D+1}(\mathbf{p}) = 1$, and the $v_d(\mathbf{p})$ functions are orthonormal for $d = 1, ..., (D + 1)$.

Definition 2. (Affine TP model). The model (8) is called an Affine TP model if the matrix $\mathbf{S}(\mathbf{p})$ is given as

$$\mathbf{S}(\mathbf{p}) = \mathcal{S}^{aff} \bigboxtimes_{k=1}^{K} \mathbf{v}^{(k)}(\mathbf{p}^{(k)}), \quad (14)$$

in which the $\mathcal{S}^{aff}$ core tensor is on $\mathbb{S}$ as $\mathcal{S}^{aff} \in \mathbb{S}^{(D_1+1)\times\cdots\times(D_K+1)}$, the D_k $(k = 1..K)$ values are called k-mode dimensions, and its expansion

$$\mathbf{S}(\mathbf{p}) = \sum_{d=1}^{D_k+1} \left(\mathcal{S}^{aff}_{d_k=d} \bigboxtimes_{l=1,l\neq k}^{K} \mathbf{v}^{(l)}(\mathbf{p}^{(l)}) \right) v_d^{(k)}(\mathbf{p}^{(k)}) \quad (15)$$

is ASVD with $\sigma_1^{(k)}, ..., \sigma_{D_k}^{(k)}$ for each k.

Based on this form, the (11) Polytopic TP model can be obtained by determining enclosing polytopes for all $\mathbf{v}^{(k)}(\mathbf{p}^{(k)})$ trajectories in the D_k dimensional spaces for all $k = 1..K$. For more details, see Kuti et al. (2017b,a); Kuti and Galambos (2018); Kuti et al. (2017c).

3. MAIN RESULTS

3.1 Derivation of the qLPV model

First consider the continuous time LTI dynamics of the PK-PD processes. By defining the state variables as difference from the desired equilibrium state, we can obtain the following description

$$\begin{aligned}
\dot{q}_1 &= -(k_{10} + k_{12} + k_{13})q_1 + k_{21}q_2 + k_{31}q_3 + u/V_1,\\
\dot{q}_2 &= k_{12}q_1 - k_{21}q_2,\\
\dot{q}_3 &= k_{13}q_1 - k_{31}q_3,\\
\dot{q}_4 &= -k_d q_4 + k_a q_1,
\end{aligned}$$

where $q_4 = C_e - C_{ed}$.

Then the nonlinear saturation, and the dynamics of the sensor can be realized as

$$\begin{aligned}
\dot{q}_5 &= -q_6 + \alpha q_4 + d(t),\\
\dot{q}_6 &= -0.1841[s^{-1}]q_6 + 0.0115[s^{-1}]q_5,
\end{aligned}$$

where

$$\alpha = -\frac{E_{max}C_{E50}^{\gamma}}{(C_{E50}^{\gamma} + C_{ed}^{\gamma})(C_{E50}^{\gamma} + C_e^{\gamma})} \frac{C_e^{\gamma} - C_{ed}^{\gamma}}{C_e - C_{ed}}, \quad (16)$$

$$C_{ed} = C_{E50} \sqrt[\gamma]{\frac{E_0 - 50}{E_{max} - E_0 + 50}}. \quad (17)$$

By writing it in the form

$$\dot{\mathbf{q}} = \mathbf{A}_0(\mathbf{p})\mathbf{q} + \mathbf{B}_{u0}u + \mathbf{B}_{d0}d, \quad (18)$$

its behaviour in the sampling time can be written as a discrete-time model

$$\begin{aligned}
\mathbf{x}_{1:6}(T + 1) = e^{\mathbf{A}_0(\mathbf{p})T_s}\mathbf{x}_{1:6}(T) +\\
+ \Gamma(\mathbf{p})\mathbf{B}_{u0}u(T) + \Gamma(\mathbf{p})\mathbf{B}_{d0}d(T), \quad (19)
\end{aligned}$$

where

$$\Gamma(\mathbf{p}) = \int_{\tau=0}^{T_s} e^{\mathbf{A}_0(\mathbf{p})\tau} d\tau. \quad (20)$$

Then the time-delay $T_d = kT_s$ can be taken into account by applying k state variables as

$$x_{6+i}(T + 1) = x_{6+i-1}(T), \quad (21)$$

where $i = 1, .., k$.

Finally, state variables of the PID controller are

$$x_{6+k+1}(T + 1) = T_s x_{6+k}(T) + x_{6+k+1}(T), \quad (22)$$

$$x_{6+k+2}(T + 1) = x_{6+k}(T). \quad (23)$$

Then the $\mathbf{A}(\mathbf{p})$, $\mathbf{B}_u(\mathbf{p})$ and $\mathbf{B}_d(\mathbf{p})$ matrices of the LPV model (8) can be written as

$$\mathbf{A}(\mathbf{p}) = \begin{bmatrix}
e^{\mathbf{A}_0(\mathbf{p})T_s} & \mathbf{0}^6 & \dots & \mathbf{0}^6 & \mathbf{0}^6 & \mathbf{0}^6 & \mathbf{0}^6\\
0\ 0\ 0\ 0\ 0\ 1 & 0 & \dots & 0 & 0 & 0 & 0\\
0\ 0\ 0\ 0\ 0\ 0 & 1 & \dots & 0 & 0 & 0 & 0\\
\vdots\ \vdots\ \vdots\ \vdots\ \vdots\ \vdots & \vdots & \ddots & \vdots & \vdots & \vdots & \vdots\\
0\ 0\ 0\ 0\ 0\ 0 & 0 & \dots & 1 & 0 & 0 & 0\\
0\ 0\ 0\ 0\ 0\ 0 & 0 & \dots & 0 & T_s & 1 & 0\\
0\ 0\ 0\ 0\ 0\ 0 & 0 & \dots & 0 & 1 & 0 & 0
\end{bmatrix}, \quad (24)$$

$$\mathbf{B}_u(\mathbf{p}) = \begin{bmatrix} \Gamma(\mathbf{p})\mathbf{B}_{u0} \\ \mathbf{0}^{k+2} \end{bmatrix}, \quad \mathbf{B}_d(\mathbf{p}) = \begin{bmatrix} \Gamma(\mathbf{p})\mathbf{B}_{d0} \\ \mathbf{0}^{k+2} \end{bmatrix}. \quad (25)$$

The control signal $u(t)$ will be computed as

$$u(T) = \underbrace{[P(\mathbf{p})\ I(\mathbf{p})\ D(\mathbf{p})]}_{\mathbf{K}(\mathbf{p})} \underbrace{\begin{bmatrix} x_{6+k}(T) - r(T) \\ x_{7+k}(T) \\ (x_{6+k}(T) - x_{8+k}(T))/T_s \end{bmatrix}}_{\mathbf{y}(T)}, \quad (26)$$

in this way, the measured output of the system is

$$\mathbf{y}(T) = \begin{bmatrix} y_P(T) \\ y_I(T) \\ y_D(T) \end{bmatrix} = \underbrace{\begin{bmatrix} 0 & \dots & 0 & 1 & 0 & 0 \\ 0 & \dots & 0 & 0 & 1 & 0 \\ 0 & \dots & 0 & 1/T_s & 0 & -1/T_s \end{bmatrix}}_{\mathbf{C}} \mathbf{x}(T) + \\ + \begin{bmatrix} -1 \\ 0 \\ 0 \end{bmatrix} r(T). \quad (27)$$

The derived qLPV model is an exact description of the model detailed in subsection 2.1 including the sampling time and the time-delay. The parameters of the model are

- (non-accessible) E_0, E_{max}, C_{E50}, C_e, γ,
- (known) *weight*, *age*, *height*.

3.2 Derivation of Polytopic TP model

Three parameter sets can be distinguished:

- (E_0, E_{max}, C_{E50}, C_e, γ): influence only α, non-accessible.
- (*weight*, *height*): influence only k_{10}, exactly known.
- (*age*): influence only k_{21}, k_{12}, exactly known.

For sake of simplicity, consider k_{10}, α, and *age* as parameters. Then the following polytopic TP model can be obtained:

$$\begin{aligned}
[\mathbf{A}(\mathbf{p})\ \mathbf{B}_u(\mathbf{p})\ \mathbf{B}_d(\mathbf{p})] = \mathcal{S} \times_1 \mathbf{w}^{(1)}(\alpha)\\
\times_2 \mathbf{w}^{(2)}(k_{10}) \times_3 \mathbf{w}^{(3)}(age). \quad (28)
\end{aligned}$$

3.3 Optimisation of PID gains

Consider a controller

$$u = \mathbf{K}(\mathbf{p})\mathbf{y}, \quad (29)$$

where $\mathbf{K}(\mathbf{p})$ gains can be

– static gain as $\mathbf{K}(\mathbf{p}) = [P\ I\ D]$,
– parallel distributed polytopic TP form with single multiplicities

$$\mathbf{K}(\mathbf{p}) = \mathcal{K} \times_1 \mathbf{w}^{(2)}(k_{10}) \times_2 \mathbf{w}^{(3)}(age), \quad (30)$$

– or on higher multiplicities as

$$\mathbf{K}(\mathbf{p}) = \mathcal{K} \times_1 \mathbf{w}^{(2)}(k_{10}) \times_2 \mathbf{w}^{(2)}(k_{10}) \times_3 \mathbf{w}^{(2)}(k_{10}) \times_4 \mathbf{w}^{(3)}(age) \times_5 \mathbf{w}^{(3)}(age). \quad (31)$$

Then the closed-loop system matrix

$$\Phi(\mathbf{p}) = \mathbf{A}(\mathbf{p}) + \mathbf{B}_u(\mathbf{p})\mathbf{K}(\mathbf{p})\mathbf{C}_y \quad (32)$$

can be written as a polytopic TP form as well.

The matrix of Lyapunov function-candidate $\mathbf{X}(\mathbf{p})$ can also be structured as a polytopic TP form with arbitrary multiplicities, that depend only on the constant parameters for example

– static gain as $\mathbf{X}(\mathbf{p}) = \mathbf{X}$,
– parallel distributed polytopic TP form with single multiplicities

$$\mathbf{X}(\mathbf{p}) = \mathcal{X} \times_1 \mathbf{w}^{(2)}(k_{10}) \times_2 \mathbf{w}^{(3)}(age), \quad (33)$$

– or on higher multiplicities as

$$\mathbf{X}(\mathbf{p}) = \mathcal{X} \times_1 \mathbf{w}^{(2)}(k_{10}) \times_2 \mathbf{w}^{(2)}(k_{10}) \times_3 \mathbf{w}^{(3)}(age) \times_4 \mathbf{w}^{(3)}(age). \quad (34)$$

The definite criteria of Lemma 1 can be transformed into LMIs via method published by Kuti et al. (2017a) and solved with interior-point solvers for Lyapunov function-candidate given in a structure (as (33) or (34)) and a PID controller.

This way, for robust or gain-scheduling controllers, the stability and worst case disturbance rejection can be verified and locally optimised on the parameters P, I, D, although the static output feedback optimisation is highly non-convex.

4. NUMERICAL RESULTS

4.1 Derivation of Polytopic TP model

Considered the domain of patients, *age*, *height*, *weight*

$$age : [10, 90](year) \quad (35)$$
$$height : [140, 200](cm) \quad (36)$$
$$weight : [50, 100](kg) \quad (37)$$

and the parameter domains

$$\Omega_\alpha = [-17.6, -4.83](L/mg) \quad (38)$$
$$\Omega_{k_{10}} = [0.25, 0.69](1/min) \quad (39)$$
$$\Omega_{age} = [10, 90](year) \quad (40)$$

Considering sampling time $T_s = 1[s]$ and performing the Affine Tensor Product Model Transformation, the following approximating Affine TP model can be obtained

$$\mathbf{S}(\mathbf{p}) = \mathcal{S}^{aff} \times_1 \mathbf{v}^{(1)}(\alpha) \times_2 \mathbf{v}^{(2)}(k_{10}) \times_3 \mathbf{v}^{(3)}(age), \quad (41)$$

where dimensions of the affine descriptions are $D_1 = 1$, $D_2 = 1$ and $D_3 = 2$ and the weighting functions are depicted in Fig 1.

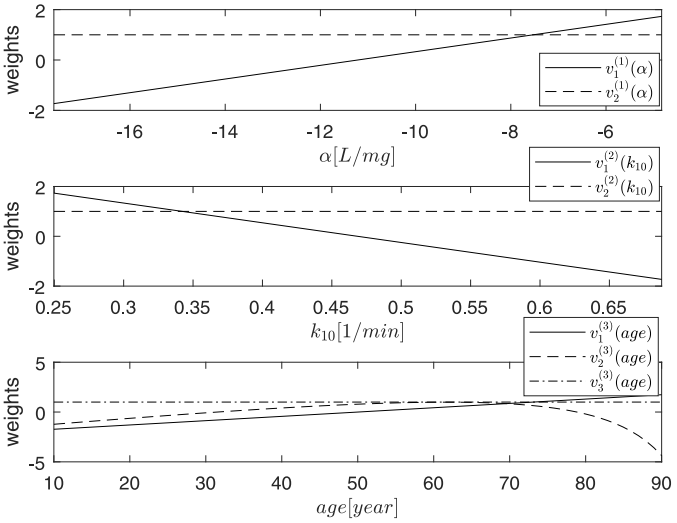

Fig. 1. The $\mathbf{v}^{(1)}(\alpha)$, $\mathbf{v}^{(2)}(k_{10})$ and $\mathbf{v}^{(3)}(age)$ weighting functions of the derived affine TP model.

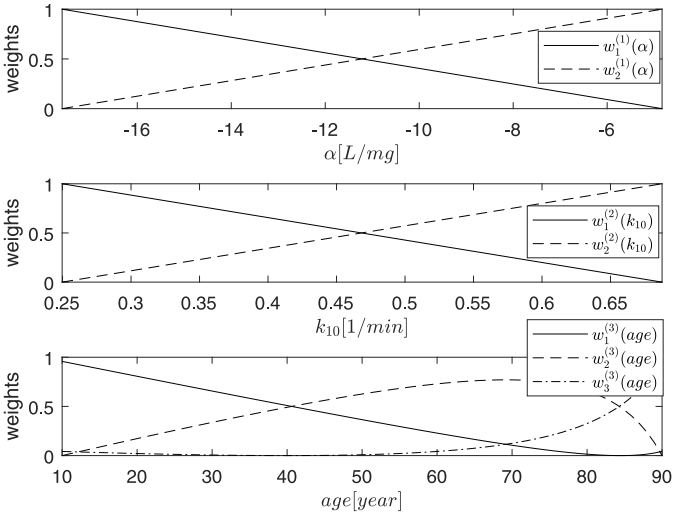

Fig. 2. The $\mathbf{w}^{(1)}(\alpha)$, $\mathbf{w}^{(2)}(k_{10})$ and $\mathbf{w}^{(3)}(age)$ weighting functions of the derived polytopic TP model.

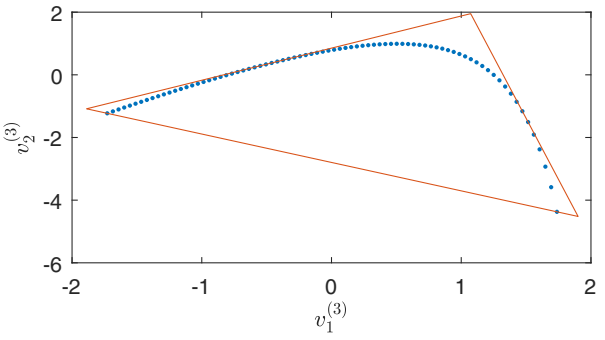

Fig. 3. The Minimal Volume Simplex enclosing polytope obtained for $\mathbf{v}^{(3)}(age)$.

By applying MVS enclosing polytopes , the polytopic model (28) can be obtained with sizes $J_1 = 2$, $J_2 = 3$, $J_3 = 2$. The corresponding weighting functions are shown in Fig. 2. The structure of the enclosing polytope constructed for $\mathbf{v}^{(2)}(\mathbf{p})$ is depicted in Fig. 3.

$m_2 \backslash m_3$	0	1	2	3
0	∞	∞	1009.4	1009.4
1	∞	∞	771.8	771.8
2	∞	∞	776.6	776.6
3	∞	∞	776.6	776.6

Table 3. Obtained γ values

For H_∞ controller design, the following filters were included into the qLPV model: A high-pass filter to the disturbance signal $d(t)$ as

$$W_d = \frac{s}{s+\omega_d}, \tag{42}$$

and a low-pass filter on the reference signal $r(t)$ written as

$$W_r = \frac{1}{s/\omega_r + 1}, \tag{43}$$

where $\omega_d = 0.3[rad/s]$ and $\omega_r = 2\pi/120[rad/s]$.

Furthermore, the integrator was chosen as performance output:

$$z(T) = \underbrace{[0\ 0\ \dots\ 0\ 0\ 0\ 1\ 0]}_{\mathbf{C}_z}\mathbf{x}(T). \tag{44}$$

4.2 Achievable performance with robust PID controller

The initial PID controller candidate was derived by naive trial and error method

$$P = 0.3, \tag{45}$$
$$I = 0.003, \tag{46}$$
$$D = -5. \tag{47}$$

To determine the overall performance with these gains, Lyapunov function candidates of the following structure were considered

$$\mathbf{X}(\mathbf{p}) = \mathcal{X} \underbrace{\times_1 \mathbf{w}^{(2)}(k_{10}) \times_2 \mathbf{w}^{(2)}(k_{10}) \cdots \times_{m_2} \mathbf{w}^{(2)}(k_{10})}_{m_2}$$
$$\underbrace{\times_{m_2+1} \mathbf{w}^{(3)}(age) \times_{m_2+2} \mathbf{w}^{(3)}(age) \cdots \times_{m_2+m_3} \mathbf{w}^{(3)}(age)}_{m_3}. \tag{48}$$

The results of the initial trial are summarized in Table 3. One can see, that $m_3 \geq 2$ is necessary to have a feasible problem, but $m_3 = 3$ does not improve the results. Similarly, although $m_2 = 1$ might enhance the performance, but by further increasing its value, numerical issues reduce the achievable performance.

Then, applying local optimisation via Nelder-Mead simplex method (see Dennis and Woods (1987)) with multiplicities $m_2 = 1$, $m_3 = 2$, it leads to gains

$$P = 0.5139, \tag{49}$$
$$I = 0.0024,$$
$$D = -6.7188,$$

the achievable performance is $\gamma = 284.0416$ that is a local minima.

4.3 Numerical simulations

The numerical simulation was performed with parameters presented in Table 2 controlled with PID gains (49). The achieved results are shown in Figure 4.

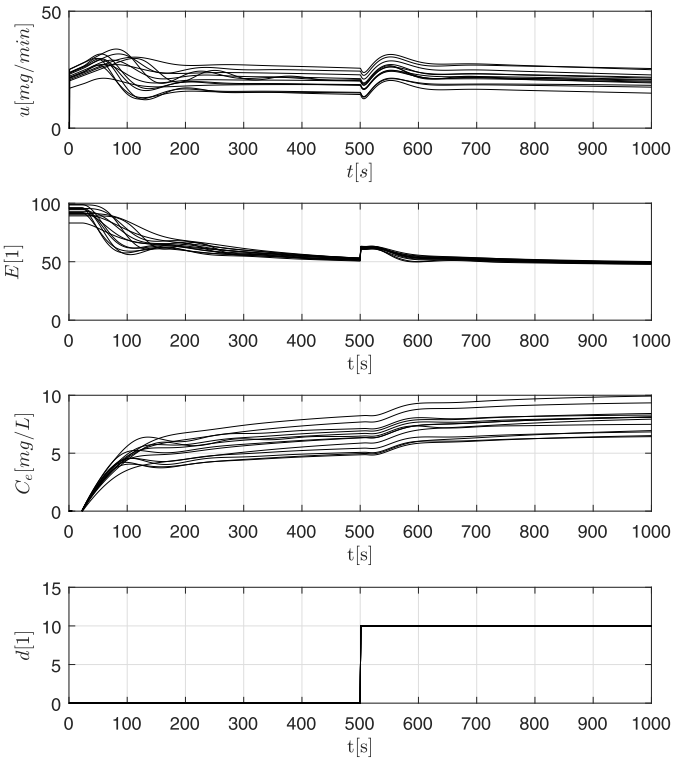

Fig. 4. Numerical simulations of controller (49) with parameters given in Table 2

The Depth of Hypnosis reaches the region $E < 60$ in 3 minutes, and the system needs one minute to eliminate the effect of disturbances.

5. CONCLUSION

The paper proposes a robust PID output feedback design method for automatic propofol administration in anesthesia. The suggested design approach utilizes the Affine Tensor Product Model Transformation to derive the polytopic TP model from the quasi-LPV system description. The so obtained polytopic model represents the closed-loop system including the controller and the dynamics of anesthetics. This model form is readily suitable for LMI-based evaluation of stability and performance, which is the main advantage of the proposed approach. As a result, within a given parameter range - that is considered in the design -, the stability and some performance characteristics are mathematically proven.

ACKNOWLEDGEMENTS

Authors thankfully acknowledge the financial support of this work by the Hungarian State and the European Union under the EFOP-3.6.1-16-2016-00010 project and by the UNKP-16-3 and UNKP-16-4 New National Excellence Program of the Ministry of Human Capacities and the support of the Doctoral School of Applied Informatics and Applied Mathematics of Óbuda University and Research and Innovation Center of Óbuda University.

REFERENCES

Baranyi, P., Yam, Y., and Varlaki, P. (2013). *Tensor Product Model Transformation in Polytopic Model-Based*

Control. Automation and Control Engineering. Taylor & Francis Group.

Bianchi, F.D., Mantz, R.J., and Christiansen, C.F. (2008). Multivariable PID control with set-point weighting via BMI optimisation. *Automatica*, 44(2), 472–478.

Bibian, S., Dumont, G.A., and Zikov, T. (2011). Dynamic behavior of bis, m-entropy and neurosense brain function monitors. *Journal of clinical monitoring and computing*, 25(1), 81–87.

Bibian, S. and Zikov, T. (2011). Neurosense® monitor with wavcns cortical quantifier.

Boyd, S.P. (1994). *Linear matrix inequalities in system and control theory*. Society for Industrial and Applied Mathematics, Philadelphia.

Crusius, C.A. and Trofino, A. (1999). Sufficient LMI conditions for output feedback control problems. *IEEE Transactions on Automatic Control*, 44(5), 1053–1057.

Dennis, J. and Woods, D.J. (1987). Optimization on microcomputers: The nelder-mead simplex algorithm. *New computing environments: microcomputers in large-scale computing*, 11, 6–122.

Dineva, A., Tar, J.K., Várkonyi-Kóczy, A., and Piuri, V. (2016). Adaptive controller using fixed point transformation for regulating propofol administration through wavelet-based anesthetic value. In *Medical Measurements and Applications (MeMeA), 2016 IEEE International Symposium on*, 1–6. IEEE.

Gahinet, P. and Apkarian, P. (1994). A linear matrix inequality approach to h∞ control. *International journal of robust and nonlinear control*, 4(4), 421–448.

Hassibi, A., How, J., and Boyd, S. (1999). A path-following method for solving BMI problems in control. In *American Control Conference, 1999. Proceedings of the 1999*, volume 2, 1385–1389. IEEE.

Hemmerling, T.M., Charabati, S., Zaouter, C., Minardi, C., and Mathieu, P.A. (2010). A randomized controlled trial demonstrates that a novel closed-loop propofol system performs better hypnosis control than manual administration. *Canadian Journal of Anesthesia/Journal canadien d'anesthésie*, 57(8), 725–735.

Ionescu, C.M., Nascu, I., and De Keyser, R. (2014). Lessons learned from closed loops in engineering: towards a multivariable approach regulating depth of anaesthesia. *Journal of clinical monitoring and computing*, 28(6), 537–546.

Kuti, J. and Galambos, P. (2018). Affine tensor product model transformation. *Complexity*. Accepted.

Kuti, J., Galambos, P., and Baranyi, P. (2017a). Control analysis and synthesis through polytopic tensor product model: a general concept. In *Proc. of the Int. Fed. of Aut. Contr. (IFAC)*, 6742–6747.

Kuti, J., Galambos, P., and Baranyi, P. (2017b). Generalization of tensor product model transformation based control design concept. In *Proceedings of the Int. Fed. of Automatic Contr. (IFAC)*, 5769–5774.

Kuti, J., Galambos, P., and Baranyi, P. (2017c). Minimal Simplex (MVS) Polytopic Model Generation and Manipulation Methodology for TP Model Transformation. *Asian Journal of Control*, 19(1), 289–301.

Lin, H.H., Beck, C., and Bloom, M. (2008). Multivariable lpv control of anesthesia delivery during surgery. In *American Control Conference, 2008*, 825–831. IEEE.

Nascu, I., Oberdieck, R., and Pistikopoulos, E.N. (2015). Offset-free explicit hybrid model predictive control of intravenous anaesthesia. In *Systems, Man, and Cybernetics (SMC), 2015 IEEE International Conference on*, 2475–2480. IEEE.

Nesterov, Y. and Nemirovsky, A. (1988). A general approach to polynomial-time algorithms design for convex programming. *Report, Central Economical and Mathematical Institute, USSR Academy of Sciences, Moscow*.

Orliaguet, G.A., Lambert, F.B., Chazot, T., Glasman, P., Fischler, M., and Liu, N. (2015). Feasibility of closed-loop titration of propofol and remifentanil guided by the bispectral monitor in pediatric and adolescent patientsa prospective randomized study. *The Journal of the American Society of Anesthesiologists*, 122(4), 759–767.

Padula, F., Ionescu, C., Latronico, N., Paltenghi, M., Visioli, A., and Vivacqua, G. (2015). A gain-scheduled pid controller for propofol dosing in anesthesia. *IFAC-PapersOnLine*, 48(20), 545–550.

Pilge, S., Zanner, R., Schneider, G., Blum, J., Kreuzer, M., and Kochs, E.F. (2006). Time delay of index calculationanalysis of cerebral state, bispectral, and narcotrend indices. *The Journal of the American Society of Anesthesiologists*, 104(3), 488–494.

Qiu, J., Feng, G., and Gao, H. (2013). Static-output-feedback h_∞ control of continuous-time T-S fuzzy affine systems via piecewise Lyapunov functions. *IEEE Transactions on Fuzzy Systems*, 21(2), 245–261.

Tar, J.K., Rudas, I.J., Nádai, L., Felde, I., and Csanádi, B. (2016). Tackling complexity and missing information in adaptive control by fixed point transformation-based approach. In *Systems, Man, and Cybernetics (SMC), 2016 IEEE International Conference on*, 001519–001524. IEEE.

Thevenet, J.b., Noll, D., and Apkarian, P. (2004). Nonlinear spectral SDP method for BMI-constrained problems: Applications to control design. In *in Proceedings ICINCO*.

Van Heusden, K., Dumont, G.A., Soltesz, K., Petersen, C.L., Umedaly, A., West, N., and Ansermino, J.M. (2014). Design and clinical evaluation of robust pid control of propofol anesthesia in children. *IEEE Transactions on Control Systems Technology*, 22(2), 491–501.